

AD-A046 310

STANFORD RESEARCH INST MENLO PARK CALIF

F/6 17/5

ASSESSMENT OF SOME MECHANISMS FOR NEAR IR NARROW PASS-BAND FILT--ETC(U)

OCT 77 J W CHAMBERLAIN, M A RUDERMAN

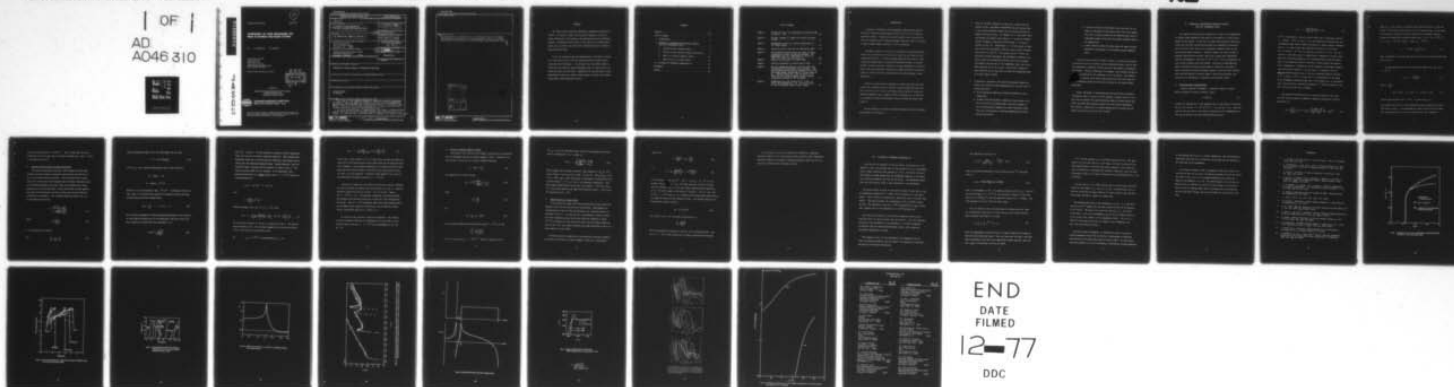
DAHC15-73-C-0370

NL

UNCLASSIFIED

SRI-JSR-76-31

1 OF 1  
AD  
A046 310



AD A046310

JASO

Technical Report JSR-76-31

October 1977

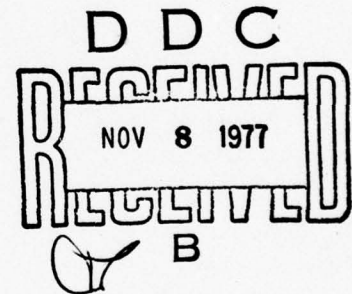
12  
B.S.

## ASSESSMENT OF SOME MECHANISMS FOR NEAR IR NARROW PASS-BAND FILTERS

By: J. W. CHAMBERLAIN M. A. RUDERMAN

Contract DAHC15-73-C-0370  
ARPA Order No. 2504  
Program Code No. 3K10  
Date of Contract: 2 April 1973  
Contract Expiration Date: 30 November 1977  
Amount of Contract: \$3,176,255

Approved for public release; distribution unlimited



Sponsored by

DEFENSE ADVANCED RESEARCH PROJECTS AGENCY  
1400 WILSON BOULEVARD  
ARLINGTON, VIRGINIA 22209



STANFORD RESEARCH INSTITUTE  
Menlo Park, California 94025 • U.S.A.

The views and conclusions contained in this document are those of the authors and should not be interpreted as necessarily representing the official policies, either expressed or implied, of the Defense Advance Research Projects Agency, or the U.S. Government.

UNCLASSIFIED

SECURITY CLASSIFICATION OF THIS PAGE (When Data Entered)

REPORT DOCUMENTATION PAGE		READ INSTRUCTIONS BEFORE COMPLETING FORM
1. REPORT NUMBER JSR-76-31	2. GOVT ACCESSION NO.	3. RECIPIENT'S CATALOG NUMBER
4. TITLE (and Subtitle) <b>ASSESSMENT OF SOME MECHANISMS FOR NEAR IR NARROW PASS-BAND FILTERS.</b>		5. TYPE OF REPORT & PERIOD COVERED <b>TECHNICAL REPORT</b>
7. AUTHOR(s) <b>J.W. Chamberlain and M.A. Ruderman</b>		6. PERFORMING ORG. REPORT NUMBER <b>SRI-JSR-76-31</b>
9. PERFORMING ORGANIZATION NAME AND ADDRESS SRI, International 1611 North Kent Street Arlington, VA 22209		8. CONTRACT OR GRANT NUMBER(s) <b>DAHC15-73-C-0370</b>
11. CONTROLLING OFFICE NAME AND ADDRESS Advanced Research Projects Agency 1400 Wilson Boulevard Arlington, Virginia 22209		10. PROGRAM ELEMENT, PROJECT, TASK AREA & WORK UNIT NUMBERS <b>12 34 p.</b>
14. MONITORING AGENCY NAME & ADDRESS (if diff. from Controlling Office)		12. REPORT DATE <b>Oct 1977</b>
		13. NO. OF PAGES <b>21</b>
		15. SECURITY CLASS. (of this report) <b>UNCLASSIFIED</b>
		15a. DECLASSIFICATION/DOWNGRADING SCHEDULE
16. DISTRIBUTION STATEMENT (of this report)  <b>APPROVED FOR PUBLIC RELEASE; DISTRIBUTION UNLIMITED</b>		
17. DISTRIBUTION STATEMENT (of the abstract entered in Block 20, if different from report)		
18. SUPPLEMENTARY NOTES		
19. KEY WORDS (Continue on reverse side if necessary and identify by block number)  <b>CARBON DIOXIDE IR FILTERS</b>		
20. ABSTRACT (Continue on reverse side if necessary and identify by block number) <b>Two types of novel physical systems are examined as possible IR filters. To observe a small, hot CO<sub>2</sub> source against a cooler but strong background of CO<sub>2</sub> emission, the background must be exceedingly uniform. An optically thick filter of CO<sub>2</sub> can turn a variable background into a uniform one, while still transmitting the hot signal at high rotational lines. At the IR absorption edge of semiconductors, the index of refraction could theoretically (for the proper materials) exhibit abrupt variations with wave-length. If a material had a specified index of refraction only within a narrow</b>		

DD FORM 1473  
1 JAN 73  
EDITION OF 1 NOV 65 IS OBSOLETE

332 500 UNCLASSIFIED  
SECURITY CLASSIFICATION OF THIS PAGE (When Data Entered)

mt

UNCLASSIFIED

SECURITY CLASSIFICATION OF THIS PAGE (When Data Entered)

19. KEY WORDS (Continued)

20. ABSTRACT (Continued)

wavelength band, it could serve as an effective filter for that band. Examination of the qualities of real semiconductors does not, however, hold promise for their use in developing finely tuned adjustable filters.

ACCESSION for	
NTIS	Write Section <input checked="" type="checkbox"/>
DDC	DDC Section <input type="checkbox"/>
UNCLASSIFIED	<input type="checkbox"/>
J. Z. BARTON	
BY	
DISTRIBUTION/AVAILABILITY CODES	
Dist. A ALL GROUPS SPECIAL	
A	



# ABSTRACT

Two types of novel physical systems are examined as possible IR filters. To observe a small, hot  $\text{CO}_2$  source against a cooler but strong background of  $\text{CO}_2$  emission, the background must be exceedingly uniform. An optically thick filter of  $\text{CO}_2$  can turn a variable background into a uniform one, while still transmitting the hot signal at high rotational lines.

At the IR absorption edge of semiconductors, the index of refraction could theoretically (for the proper materials) exhibit abrupt variations with wavelength. If a material had a specified index of refraction only within a narrow wavelength band, it could serve as an effective filter for that band. Examination of the qualities of real semiconductors does not, however, hold promise for their use in developing finely tuned adjustable filters.

## CONTENTS

ABSTRACT . . . . .	iii
LIST OF FIGURES . . . . .	v
I INTRODUCTION . . . . .	1
II THEORETICAL SEMICONDUCTOR REFRACTION INDICES NEAR THE "FUNDAMENTAL EDGE" . . . . .	4
A. Refraction Near Idealized Edge . . . . .	4
B. Effects of Electron-Hole Coulomb Interaction . .	7
C. Effect of External Magnetic Fields . . . . .	11
D. Edge Structure in Large Fields . . . . .	12
III FILTERING BY RESONANCE ABSORPTION (U) . . . . .	15
REFERENCES . . . . .	19
FIGURES . . . . .	20

## LIST OF FIGURES

Figure 1	Theoretical fit to the experimental absorption edge of InSb at $-5^{\circ}\text{K}$ . . . . .	20
Figure 2	Spectral response of InGaSb for various fractions of InSb . . . . .	21
Figure 3	Transmission curves for various compositions of the InGaSb system . . . . .	22
Figure 4	Form parta for $Rl\ n(X)$ near an "absorption edge" . .	23
Figure 5	The continuum exciton peak at the onset of direct transitions is shown for gallium arsenide. The measurements are for temperatures of $294^{\circ}\text{K}$ ( $\circ$ ) $180^{\circ}\text{K}$ ( $\square$ ), $90^{\circ}\text{K}$ ( $\triangle$ ), and $21^{\circ}\text{K}$ ( $\circ$ ) . . . . .	24
Figure 6	Indices of Refraction for a Model Edge . . . . .	25
Figure 7	Impurity broadening of exciton peak in GaSb . . . .	26
Figure 8	Detailed magneto-absorption traces for $E  B$ with the magnetic field intensity as a parameter. The lowest energy exciton line is shown in (a) at $77^{\circ}\text{K}$ . The higher energy transitions at $77^{\circ}\text{K}$ are shown in (b). Similar traces for $1.5^{\circ}\text{K}$ are shown in (c) where the first exciton begins to show a double transmission minimum at 38.9 kilogauss . . . . .	27
Figure 9	Transmission of a $\text{CO}_2$ Filter at $P = 1\text{ atm}$ , $T = 200^{\circ}\text{K}$ , and thickness of 1 cm. The curves refer to three rotational lines in the R branch . . . . .	28

## I INTRODUCTION

A variety of scientific and technological applications would be served by a very narrow band-pass IR filter ( $10^{-2}$  to  $10^{-3}$   $\mu$ ) with an adjustable window. Usually devices which satisfy such criteria do so only for extremely well collimated incident beams and tend to fail when a large incident angular aperture ( $\sim 45^\circ$ ) is required.

The DARPA program for filters is, at present, being actively negotiated with contractors, and we have not been privy to details of any contemplated devices. A survey briefing indicated that there is still a major gap between what is presently achievable and what is desired. We have, as far as we know, looked only at some possibilities quite different from those presently considered by DARPA contractors and have no reason to believe that such possibilities are more promising or even competitive.

Ideally a filter would be composed of a particular material which allows only a desired spectral interval to pass through from many incident directions, and in which the window could be moved by varying an external parameter such as magnetic field or pressure, or, in the case of a gaseous or liquid path material, even by varying the filter composition.

We have looked at two types of physical systems for their potential applications to IR filters:



1. When the incident radiation is from, say, a distant hot  $\text{CO}_2$  gaseous source, atmospheric ( $200\text{--}300^\circ\text{K}$ )  $\text{CO}_2$  will blanket most of its spectral emission except for that associated with the highest rotational lines. For example, at a "line width" halfway between two adjacent line centers,  $J = 10$  has an overhead optical thickness of 300 above 30 km whereas  $J = 70$  has an opacity of only .07. Nevertheless,  $J = 70$  will appear in emission outside the atmosphere, since the total optical thickness above ground is about 10. Cold gaseous  $\text{CO}_2$  in a filter can effectively absorb atmospheric  $\text{CO}_2$  fundamental radiation, and allow to pass the vibrational overtones and the very highly rotationally excited part of the fundamental from a hot source while emitting little of its own. This "filter" appears to have potential use in some cases in which the background needs to be made highly uniform.
2. In principle, insulators with narrow energy gaps between the valence and conduction bands (semiconductors) can have the following properties:
  - The IR absorption edge has an energy determined by alloy composition.
  - Coulomb attraction between a conduction electron and a valence hole gives the absorbed edge a structure similar to that of photoelectric emission in atoms: absorption lines below the continuum and a continuum beginning with finite photon absorptivity.

- A rapidly varying and potentially large real part for the index of refraction of such matter very close to an absorption line or edge if impurities and imperfections could be suppressed enough to keep the line widths extremely small at low temperatures.
- A small effective mass ( $m^*$ ) which makes the edge structure sensitive to variations in an externally applied magnetic field.

If matter could be made in which an index of refraction approached a particular value only within a narrow wavelength window, then an optical system may be designed in which only that wavelength is transmitted and focused. Critical reflection, for example, could perhaps be made an effective reflector for all radiation not in the window. Even making a mass of such matter could defocus and diffuse over the focal plane all source radiation except that from point sources at the chosen window wavelength.

"Normal specimens" of semiconductors have sufficiently broadened "fundamental edge" structure that the observed averaged index of refraction does not exhibit the large variations which are theoretically possible, and this makes present prospects for such filters pessimistic. Even ideally, temperatures of several degrees would be needed and the window would be much less than  $10^{-3}$  eV wide.

## II THEORETICAL SEMICONDUCTOR REFRACTION INDICES NEAR THE "FUNDAMENTAL EDGE"

The rapidly varying index of refraction of a gas in the neighborhood of visible atomic absorption line might be the basis for a filter with a window in that region. In the near IR region where molecular vibrations rather than electron transitions determine the fundamental frequencies, such refraction index effects are very greatly reduced because of the large nuclear masses involved. Secondly, despite the large variety of possible molecules and isotopes, they do not really give "adjustable" relevant wavelengths on the scale of  $10^{-2}$  to  $10^{-3}$   $\mu$  or the possibility of very rapidly changing the filter window. Electrons in semiconductors might conceivably contribute large index of refraction variations at fairly arbitrarily chosen wavelengths because of the very small electron mass (and even smaller "effective mass"), high electron density, and sensitivity of parameters to composition and external fields.

### A. Refraction Near Idealized Edge

A typical measured "fundamental absorption" edge for "direct" photon absorption is given in Figure 1 where

$$\alpha = \frac{2\pi}{\lambda} \text{Im } n \quad (1)$$

relates the absorptivity to the imaginary part of the index of refraction. For  $h\nu = 0.3$  eV,  $\alpha h\nu \sim 2 \cdot 10^3$   $\text{cm}^{-1}$  eV,  $\lambda \sim 4\mu$ , and  $\text{Im } n \sim 0.4$ . The variation of the real part of the index of refraction in the neighborhood of the edge is given by the usual Kramers-Kronig relation



$$\operatorname{Re} n - 1 = \frac{2P}{\pi} \int_0^{\infty} \frac{\operatorname{Im} n(\omega')}{\omega'^2 - \omega^2} \omega' d\omega' \quad (2)$$

If  $\operatorname{Re} n$  is required to vary by several tenths over a wavelength interval  $\Delta\lambda \sim \text{several} \cdot 10^{-3} \mu$  at, say,  $\lambda = 4\mu$ , then Equation (2) implies that the "fundamental edge" must be almost precisely at a photon energy corresponding to  $\lambda = 4\mu$  and it must have resolvable structure in it in which  $\Delta\operatorname{Im} n \geq \text{several} \cdot 10^{-1}$  over an interval  $\Delta\lambda \lesssim \text{several} \cdot 10^{-3} \mu$ . The sensitivity of the edge energy to composition is suggested by Figure 2 which gives the transition probability for lifting electrons from the valence band to the conduction band as a function of photon energy and semiconductor composition. Transmission curves measured at much higher temperatures are given in Figure 3. In both cases it is apparent that the measured material does not have a vertical absorption edge on the scale of  $\Delta\lambda \sim \text{several} \cdot 10^{-3} \mu$ . We turn next to a consideration of the shape of the fundamental absorption edge and of the related  $\operatorname{Re} n$ , if all impurities, lattice defects, carriers and phonons ( $T \sim 0^\circ\text{K}$ ) were absent and the ideal theoretical shape was achievable.

The theoretical absorptivity for a valence-conduction band transition for which no phonon is needed for momentum conservation ("direct" transition) is

$$\alpha_0 = \frac{2e^2}{n_0 c m^2 \omega} \left| \langle c | \hat{e} \cdot \vec{p}_{12} | v \rangle \right|^2 \left( \frac{2m_v m_c}{m_v + m_c} \right)^{3/2} (\hbar\omega - E_g)^{1/2} \quad (3)$$



where  $m_{v,c}$  is the valence, conduction band "effective mass,"  $E_g$  the gap energy,  $\hat{e}$  the photon polarization,  $m$  the free electron mass,  $n_0$  the index of refraction,  $\langle c | \vec{p}_{12} | v \rangle$  the matrix element of the momentum operator between the valence and conduction bands, and  $\omega = 2\pi\nu$ . For  $\omega \sim 10^{15} \text{ s}^{-1}$ ,  $n_0 \sim 3$ ,  $m_{v,c} \sim 10^{-1} m$ ,  $\langle c | \vec{p}_{12} | v \rangle \sim \hbar/a_0$ ,  $a_0 \sim 10^{-8} \text{ cm}$ ,

$$\alpha_0 \sim 3 \cdot 10^4 (1 - E_g/\omega)^{1/2} \text{ cm}^{-1} . \quad (4)$$

This  $\omega$ -dependence of the gap edge is well fitted to the measured InSb edge data in Fig. 1.

For the absorptive part of the refraction index of Eq. (4), with  $\omega \sim 10^{15} \text{ s}^{-1}$ ,

$$\text{Rl } n - 1 \sim \frac{x^{3/2} f(x)}{2} \quad (5)$$

with  $x \equiv \frac{\hbar\omega}{E_g}$ ,

$$f(x) = x^{-2} [2 - (1+x)^{1/2} - (1-x)^{1/2} \theta(1-x)] , \quad (6)$$

and the step function  $\theta(y) = 1$  for  $y > 0$  and 0 for  $y < 0$ .

The singular part of  $\text{Rl } n$  at the absorption edge is given by the cusp of  $f(x)$  shown in Fig. 4. The magnitude and width of the cusp do not give very great variations in  $\text{Rl } n$  even close to the cusp. Equations

(5) and (6) give  $d/dx R\ell n \sim \frac{1}{2}(1-x)^{-\frac{1}{2}}$ . Fig. 4 shows that the total variations in  $R\ell n$  is less than 0.2 and  $\Delta R\ell n$  between say 1 and  $2 \cdot 10^{-3} \mu$  of the edge is only  $10^{-2}$ .

#### B. Effects of Electron-Hole Coulomb Interaction

The idealized absorption edge has a much changed structure when coulomb attraction between a conduction band electron and the hole it left in the valence band is included. The hole-electron pair interaction can form loosely bound hydrogen-like structures (excitons) which give discrete absorption lines just below the continuum and a finite absorption at the continuum edge. (These effects may be most apparent when there are sufficiently few free carriers that the hole-electron attraction is unscreened.) The continuum absorption edge of Eq. (3) is multiplied by the factor

$$f = \frac{2\pi R^{\frac{1}{2}}(\hbar\omega - E_g)^{\frac{1}{2}}}{1 - \exp\left(\frac{-2\pi R^{\frac{1}{2}}}{\hbar\omega - E_g}\right)} \quad (7)$$

where

$$R = \frac{m^* e^4}{2\kappa^2 \hbar^2}, \quad (8)$$

$\kappa$  is the dielectric constant,

and

$$\frac{1}{m^*} = \frac{1}{m_v} + \frac{1}{m_c}. \quad (9)$$

Then the absorption edge of Eq. (4) would begin with the jump

$$\alpha \sim 3 \cdot 10^4 2\pi(R/E_g)^{1/2} \quad (10)$$

at  $\hbar\omega = E_g$ . For a typical semiconductor with a near IR gap and

$$m^* \sim .03m, \kappa \sim 15,$$

$$R \sim \text{several} \cdot 10^{-3} \text{ eV}.$$

Therefore  $\alpha$  at the fundamental edge  $\sim 10^4 \text{ cm}^{-1}$ . In addition, below the edge, there is a hydrogen-like spectrum of absorption lines from bound electron-hole pairs with binding energy

$$E_B = -\frac{R}{\hat{n}^2}, \quad \hat{n} = 1, 2, \dots, \infty. \quad (11)$$

The oscillator strengths for photon absorption resulting in the creation of such lines is proportional to the probability that the electron and hole (exciton) are found with zero separation, i.e.,

$$|\phi(0)|^2 = \frac{m^{*3} e^6}{\pi \hat{n}^3 \hbar^6 \kappa} \quad (12)$$

For  $m^*/m \sim .03$  and  $\kappa \sim 15$  this oscillator strength is hugely suppressed below its value for an optical electron transition. When averaged over absorption lines the  $\alpha$  from the discrete absorption lines merges continuously into the continuum absorption edge. Typical measured  $\alpha$  near the absorption edge, including exciton creation, is shown in Fig. 5. The discrete exciton peaks are not resolved. If we approximate this unresolved structure as a single exciton line  $R \sim 3 \cdot 10^{-3}$  eV below the continuum edge with

$$\int \alpha d\epsilon \sim 10^4 \text{ cm}^{-1} \cdot 3 \cdot 10^{-3} \text{ eV}$$

and

$$\alpha = \left( \frac{\hbar \omega}{E_g} \right) 10^4 \text{ cm}^{-1}$$

beyond the edge, up to, say,  $\hbar \omega = E_1 \sim 2 \text{ eV}$ , then

$$R \ell n - 1 \sim \frac{R c \cdot 10^4 \text{ cm}^{-1}}{\pi \omega_g (\hbar \omega - E_g + R)} + \frac{2c}{\pi \omega_g} \cdot 10^4 \text{ cm}^{-1} \ln \left| \frac{\omega_1 - \omega}{\omega_g - \omega} \right| \quad (13)$$

The qualitative behavior of the  $R \ell n$  is sketched in Fig. 6. The approximations leading to Eq. (13) certainly exaggerate the possible variation of  $R \ell n$  very close to the absorption edge.

For  $\omega_g \sim 5 \cdot 10^{14} \text{ s}^{-1}$  corresponding to  $\lambda_g \sim 4\mu$ ,



$$R\ell n - 1 \sim \frac{0.2R}{(\hbar\omega - E_g + R)} + 0.4 \ln \left| \frac{\omega_1 - \omega}{\omega_g - \omega} \right|. \quad (14)$$

Thus to get a rapid change in  $R\ell n$  of order unity, one must get within an energy  $R/5$  of the ground exciton state (which also has the greatest oscillator strength). The continuum singularity, if treated correctly, would merge with the infinite number of excited loosely bound exciton states for which it is the asymptote. Therefore large changes in  $R\ell n$  are not realizable when linewidths exceed  $R/5 \sim 5 \cdot 10^{-4}$  eV.

Lowering the temperature both shifts the absorption edge by changing the lattice spacing and sharpens the exciton peak as in Fig. 5. Impurity reduction reduced the width to several  $\cdot 10^{-3}$  eV in Fig. 7 where  $kT = 2 \cdot 10^{-4}$  eV. At  $T \sim 30^\circ\text{K}$  thermal broadening from phonon emission and absorption are probably sufficient to keep  $\Delta R\ell n$  from having sharp variations. Even at  $T = 0^\circ\text{K}$  broadening comes from phonon emission which can accompany photon absorption, impurities, lattice defects, varied crystal orientations when  $m^*$  is a tensor, etc.

In principle long relaxation times are achievable: the original cyclotron resonance detection by Dresselhaus, Kip, and Kittel in Ge at  $4^\circ\text{K}$  had electron and hole  $\tau \sim 5 \cdot 10^{-11}$  sec corresponding to  $\delta E \equiv \hbar/\tau \sim 10^{-5}$  eV.

### C. Effect of External Magnetic Fields

Considerable fine structure and frequency shifting can be introduced into an absorption edge by an external magnetic field. Instead of the form of Eqs. (3) and (4) for a direct allowed transition,

$$\alpha_0 = A(\hbar\omega - E_g)^{\frac{1}{2}}, \quad (15)$$

the imposition of a field B gives

$$\alpha_B = A 2^{-\frac{1}{2}} \omega_c^* \sum_n \frac{1}{(\omega - \omega_n)^{\frac{1}{2}}} \quad (16)$$

where

$$\omega_c^* = \frac{eB}{m^* c} \quad (17)$$

and

$$\omega_n = E_g + (n + \frac{1}{2}) \omega_c^*. \quad (18)$$

For the small possible electron effective mass  $m^* \sim 10^{-2} m$  in InSb

$$\frac{\omega_c^*}{\omega_g} \sim \frac{1}{30} \left( \frac{B}{10^4} \right)$$

with B in Gauss and  $\omega_g \sim 5 \cdot 10^{14} \text{ s}^{-1}$ . Then the singular part of

$\text{Re } n_B - 1$  near the absorption edge, and with the parameters that were used in obtaining Eq. (5), is given by

$$\text{Re } n_B - 1 \sim \frac{\omega_c^*}{2^{1/2} \omega_g} \sum_n \frac{\theta(1 - \omega/\omega_n)}{(1 - \omega/\omega_n)^{1/2}} \quad (19)$$

When averaged over frequency intervals large compared to  $\omega_c^*$ , Eq. (19) should reduce to the cusp part of Eqs. (5) and (6). Since  $\omega_c^*/\omega_g \leq 1/30$  for  $B \leq 10^4$  G,  $\Delta n_B$  of order unity may, in principle, be obtained only for  $\omega$  within several  $\cdot 10^{-4} \omega_n$  of one of the resonance frequencies. This again means needed widths in the near IR of several  $\cdot 10^{-4}$  eV or less. If a filter were based on the edge fine structure, shifts  $\sim 10^{-2} \mu$  could be achieved with  $\Delta B \sim 10^3$  G.

#### D. Edge Structure in Large Fields

In real matter the edge fine structure generally involves both the magnetic field and the electron-hole interactions. Measurements for transmittance by thin Ge films by Swerdling, Lax, Roth, and Button are displayed in Fig. 8. If these data are interpreted in terms of absorption only--ignoring surface reflection--then the linewidth of about  $10^{-3}$  eV or greater for both the exciton lines and the Landau transition lines of Eq. (16) would again preclude very large variations in  $\text{Re } n$  for these samples in this region.

Coulomb attraction between holes and conduction electrons dominates the Lorentz force from an external magnetic field for  $B$  sufficiently

small that

$$\hat{\rho} \equiv \left( \frac{\hbar c}{eB} \right)^{1/2} \gg a_B \equiv \frac{\hbar^2 \kappa}{m^* e^2} \quad (20)$$

or

$$B \ll B_0 \equiv \left( \frac{c e^3 m^{*2}}{\hbar^3 \kappa^2} \right) = 4 \cdot 10^9 \left( \frac{m^*}{\kappa m} \right)^2 \text{ G} . \quad (21)$$

In this sense, Cd data with  $m^* \sim .031$ ,  $\kappa = 16$ ,  $B_0 \sim 16 \cdot 10^3 \text{ G}$  do not involve "superstrong"  $B \gg B_0$ . The edge structure consists of bound excitons recognized at  $B = 0$  and the Landau quasicontinuum transitions of Eq. (16) which respond differently to varying  $B$ . But for, say, InSb with  $B_0 \sim 4 \cdot 10^3 \text{ G}$  and  $\lambda_g \sim 4\mu$ , stronger fields would begin qualitatively to change the bound exciton absorption lines. The binding energy of the ground state exciton increases

$$E_B \sim R \ln^2(a_B/\hat{\rho}) \quad (22)$$

and  $|\phi(0)|^2$  of Eq. (12) increases proportionally to

$$\frac{B}{B_0} \ln \left( \frac{B}{B_0} \right)^{1/2} .$$

This will similarly increase  $R\ell n$  and  $\text{Im } n$  at the absorption line. But for  $B \lesssim 15 \cdot 10^3 \text{ G}$  these changes do not appear qualitatively important.



In conclusion, we have not succeeded in exhibiting a reasonable parameter regime for real semiconductors which supports their fundamental absorption edge as an especially promising frequency region for the construction of finely tuned adjustable filters.

### III FILTERING BY RESONANCE ABSORPTION (U)

From outside the atmosphere we wish to detect the presence of a jet engine at, say, 9 km altitude from its  $\text{CO}_2$  emission in the  $\nu_3$  (antisymmetrical, linear vibration) band centered at 4.3  $\mu$ . The field of view of the detector is large enough that the background radiation at the detector is very much greater than that of the source. The background varies with time and position owing to real variations in the atmosphere.

The filter placed in front of the optics consists of pure  $\text{CO}_2$  at, say, 10 atmospheric pressure and  $T \approx 250^\circ\text{K}$ , with a thickness of a few centimeters. Such a filter is essentially an additional layer of natural atmosphere. (The vapor pressure for condensation of  $\text{CO}_2$  at  $250^\circ\text{K}$  is about 20 atm.) The thickness of  $\text{CO}_2$  is  $3 \times 10^{20}$  molecules/ $\text{cm}^2$  per cm of thickness, whereas that of the atmosphere is  $6 \times 10^{21}$  molecules/ $\text{cm}^2$ .

Thus the filter absorbs all the natural background radiation and thermally emits the same radiation into the detector. The only advantage provided by the arrangement is the assurance of a uniform background of emission from the controlled-environment filter, even though the terrestrial background is uneven.

Over regions of low  $J$  in the fundamental, the atmosphere and the filter are opaque everywhere and the radiation is essentially continuous and given by the Planck distribution.

The absorption coefficient is

$$k_{\nu}(J) = \frac{f(J)}{(\Delta\nu)^2 + \alpha_L^2} \cdot \frac{N S \alpha_L}{\pi} \text{ cm}^{-1}, \quad (23)$$

where the fraction absorbing in the R branch from the  $J^{\text{th}}$  rotational level is

$$f(J) = \frac{J \exp [-Bhc J (J + 1)/kT]}{\Sigma} \quad (24)$$

Here  $\nu$  is wavenumber in  $\text{cm}^{-1}$ , the damping constant at STP is  $\alpha_L = .064 \text{ cm}^{-1}$ , the band strength is  $S = 10^{-16} \text{ cm}$ , the rotational constant of the lower state is  $B = 0.3895 \text{ cm}^{-1}$ , and the partition function is  $\Sigma = kT/2Bhc$ . The line spacing is  $0.78 \text{ cm}^{-1}$  near the band origin.

The local emission when collisions keep the populations near those for thermodynamic equilibrium is  $k_{\nu} B_{\nu}$ , where  $B_{\nu}$  is the Planck function. Hence  $\text{CO}_2$  emits into space at the rate

$$I_{\nu} = \int_0^s k_{\nu} B_{\nu} e^{-k_{\nu} s} ds \sim B_{\nu} \quad (25)$$

where the approximate equality holds for constant temperature through an optically thick emitting region. Thus the lines near the peak  $J$  will emit nearly uniformly across the entire separation between adjacent lines and will appear as black-body radiation at  $250^{\circ}\text{K}$ .

At  $J \geq 60$  the emission is not uniformly optically thick. The atmospheric  $\text{CO}_2$  will then radiate to the cosmic cold with an effective line with characteristic of one-half the surface pressure. The filter will still be effective in absorbing this emission, especially since the self-broadening of  $\text{CO}_2$  is 2.2 times as effective as line broadening by  $\text{N}_2 - \text{CO}_2$  collisions.

The spectrum of a hot ( $250^\circ\text{K}$ ) source will be qualitatively different. First the "hot bands" (i.e., the 2-1, 3-2 etc. overtone bands) will be excited, and second the super position of lines at high  $J$  near the band head causes the head to appear as a sharp peak.

The R-branch band head of the fundamental  $\nu_3$  (1-0;  $\nu_0 = 2350 \text{ cm}^{-1}$ ) occurs at  $50 \text{ cm}^{-1}$  higher than the band origin and will not be obscured by the filter. The head of the first hot band (2-1;  $\nu_0 = 2325 \text{ cm}^{-1}$ ) occurs near  $J = 40$  of the fundamental, and it will be largely occulted by the filter (and, indeed, by the atmosphere itself). The 3-2;  $\nu_0 = 2300 \text{ cm}^{-1}$  band head occurs near the origin of the fundamental and will also be partially occulted.

Thus this filter arrangement, if sufficiently thick to provide a uniform background source has the distinct disadvantage of hindering observations in the sharp band heads of the hot bands. Its sole advantage would appear to be one of providing a sufficiently uniform background



by maintaining the filter at a uniform temperature, that discrimination techniques could pick out a fluctuation as arising from hot emission in the band head of the fundamental.

We conclude, therefore, with the suggestion that more accurate calculations be made (on the basis of expected parameters for the hot source, the field of view, etc.) of the signal/background ratio, where the signal is the emission at  $J \gtrsim 60$ . The effectiveness of the filter will depend in part on whether the source is strong enough to be optically thick in the far damping wings, since line separation is much greater than the line width (except near the band head) for the optically thin case.

# REFERENCES

1. J. Callaway, "Quantum Theory of the Solid State - Part B," (Academic Press, New York 1974).
2. G. Dresselhaus, A. Kip, and C. Kittel, "Cyclotron Resonance of Electrons and Holes in Silicon and Germanium Crystals," Phys. Rev. 98, 368 (1955).
3. R. Elliott, "Intensity of Optical Absorption by Excitons," Phys. Rev. 108, 1384 (1957).
4. R. Elliott, T. McLean, and G. MacFarlane, "Theory of the Effect of a Magnetic Field on the Absorption Edge in Semiconductors," Proc. Phys. Soc. LXXII, 553 (1959).
5. J. N. Howard, D. E. Burch, and D. Williams, "Infrared Transmission of Synthetic Atmospheres. II. Absorption by Carbon Dioxide," J. Opt. Soc. Amer. 46, 237-241 (1956).
6. E. Johnson, "Absorption near the Fundamental Edge," Semiconductors and Semimetals 3, 153 (1967).
7. E. Johnson and H. Fan, Phys. Rev. 139A, 1991 (1965).
8. B. Lax and J. Mavroides, "Optical Magneto Absorption," Semiconductors and Semimetals 3, 321 (1967).
9. G. N. Plass, "Spectral Emissivity of Carbon Dioxide from 1800-2500  $\text{cm}^{-1}$ ," J. Opt. Soc. Amer. 49, 821-828 (1959).
10. L. Roth, B. Lax, and S. Zwerdling, "Theory of Optical Magneto-Absorption Effects in Semiconductors," Phys. Rev. 114, 90 (1959).
11. M. Sturge, "Optical Absorption of Gallium Arsenide between 0.6 and 2.75 eV," Phys. Rev. 127, 768 (1962).
12. M. Suffczynski, "Interband Faraday Effect in Germanium," Proc. Intern. Conf. Semiconductor Phys., Prague, 1960, pp. 346-8 (1961).
13. J. Wrobel and H. Levinstein, "Photoconductivity in InSb-GaSb and InAs-GaAs Alloys," Infrared Physics 7, 201 (1967).
14. S. Zwerdling, B. Lax, L. Roth, and K. Button, "Exciton and Magneto-Absorption of the Direct and Indirect Transitions in Germanium," Phys. Rev. 114, 80 (1959).

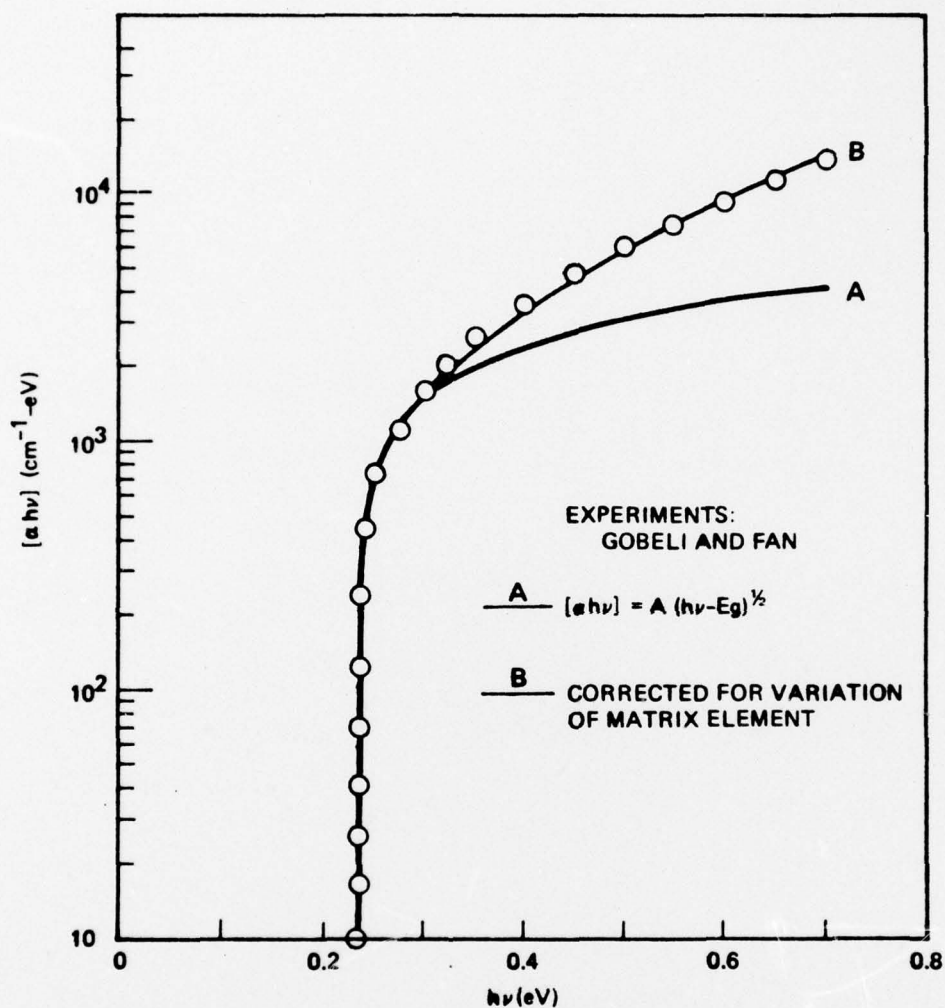


Figure 1 THEORETICAL FIT TO THE EXPERIMENTAL ABSORPTION EDGE OF InSb AT  $\sim 5^\circ\text{K}$ . (After Johnson, 1967)

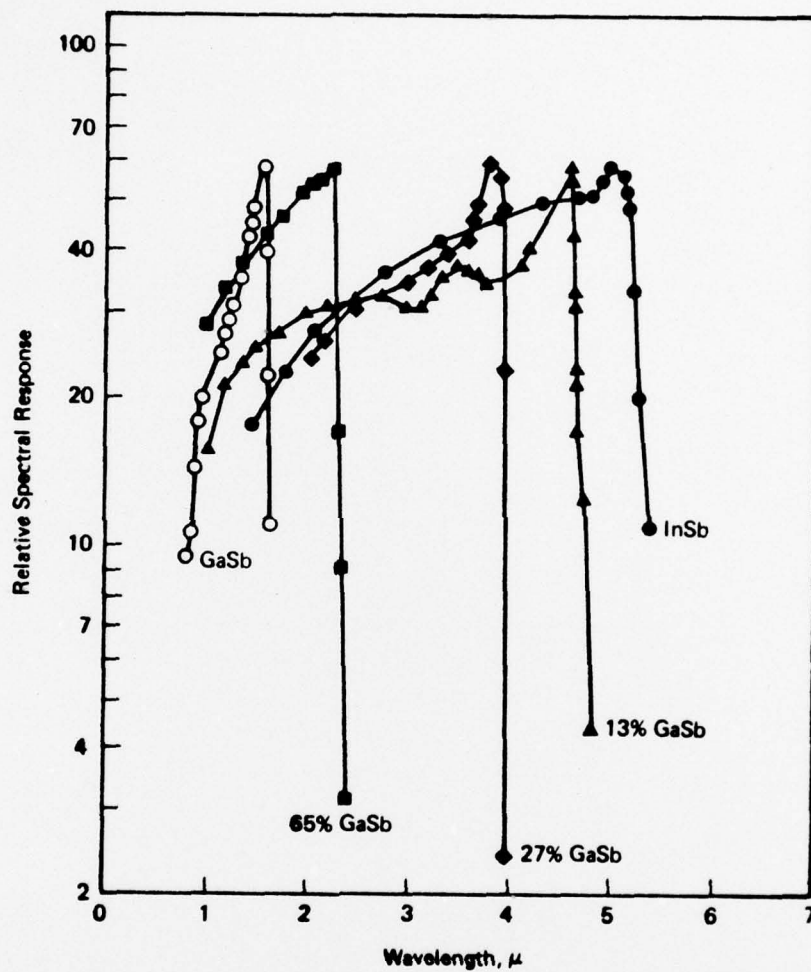


Figure 2 SPECTRAL RESPONSE OF InGaSb FOR VARIOUS FACTIONS OF InSb.  
(After Wrobel and Levinstein, 1967)



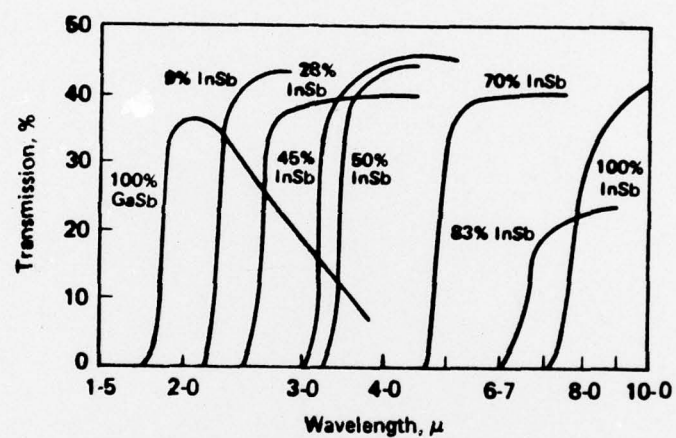


Figure 3 TRANSMISSION CURVES FOR VARIOUS COMPOSITIONS OF THE In Ga Sb SYSTEM (Wrobel and Levinstern, 1967)

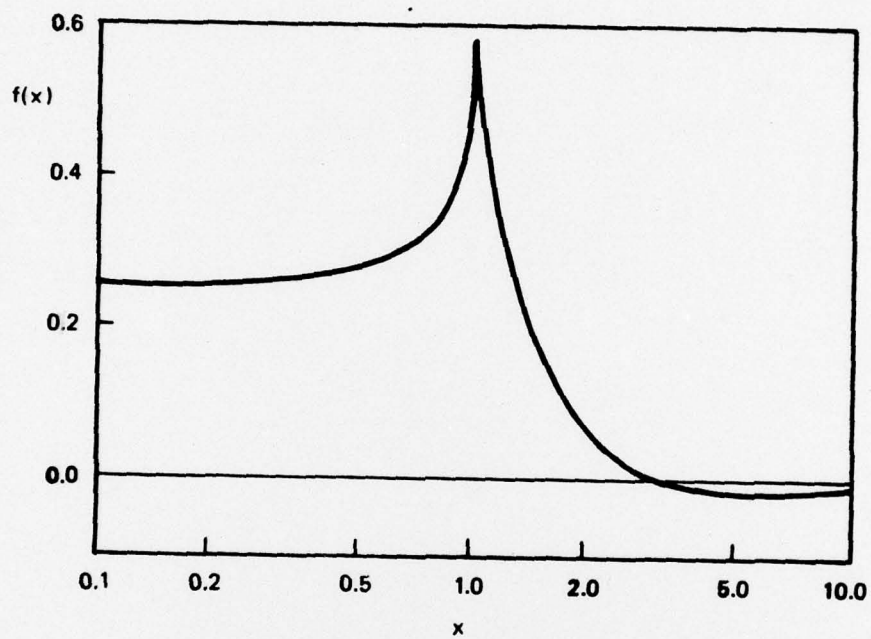


Figure 4 FORM FACTOR FOR  $Ri n(x)$  NEAR AN "ABSORPTION EDGE"  
[from Callaway (1974)]

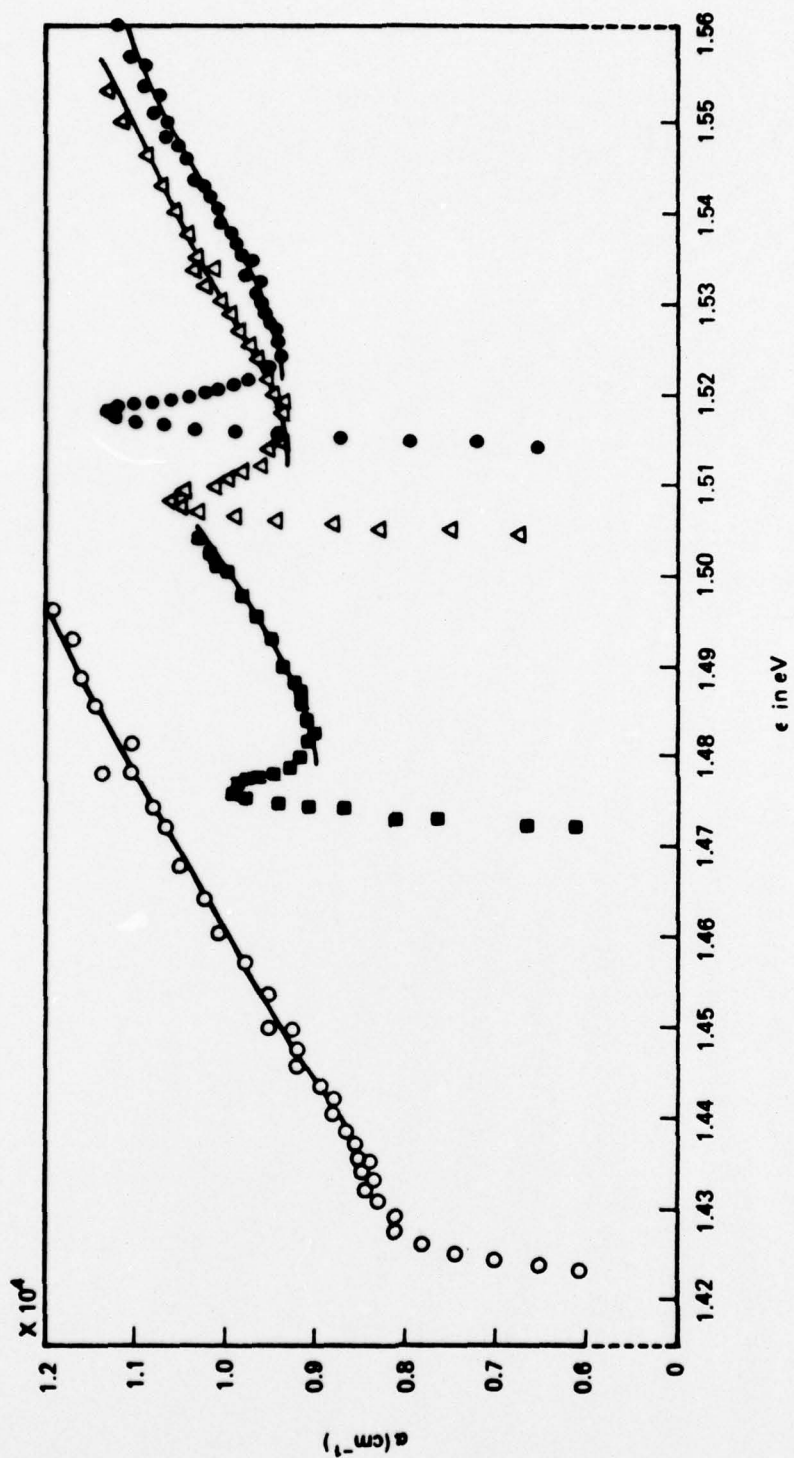


Figure 5 THE CONTINUUM EXCITON PEAK AT THE ONSET OF DIRECT TRANSITIONS IS SHOWN FOR GALLIUM ARSENIDE. THE MEASUREMENTS ARE FOR TEMPERATURES OF 294 K (○), 180 K (△), 90 K (□), AND 21 K (●) [Sturge (1962).]

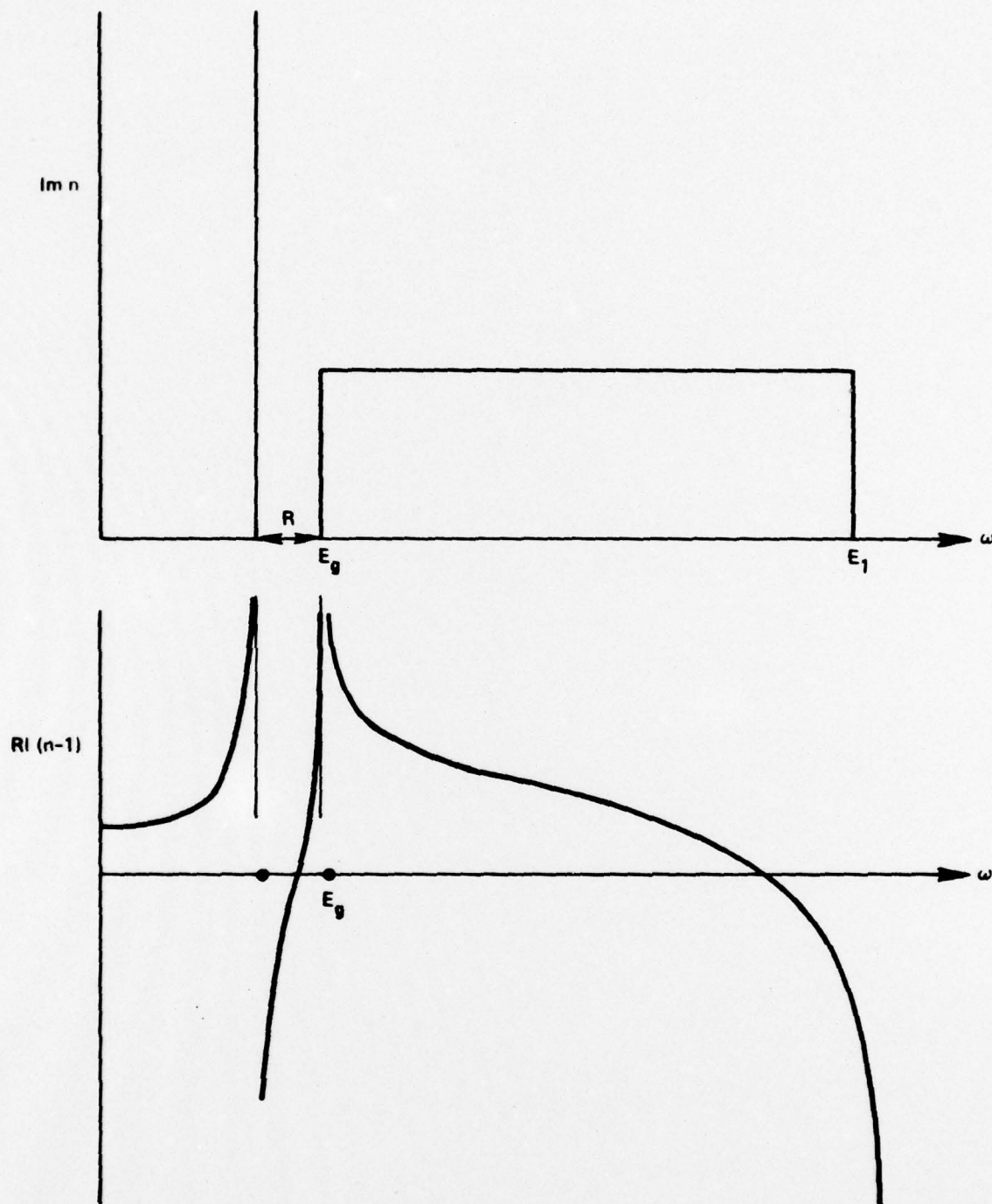


Figure 6 INDICES OF REFRACTION FOR A MODEL EDGE



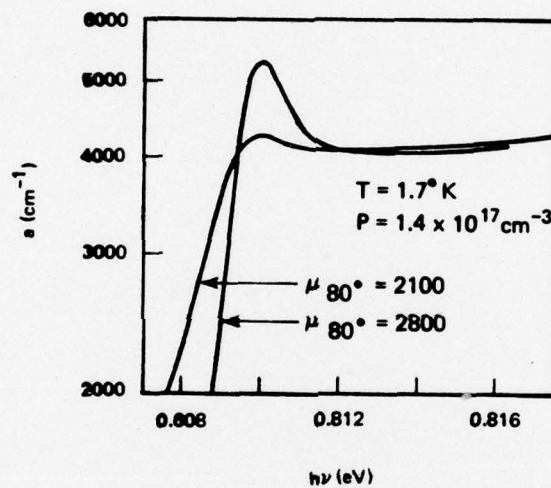
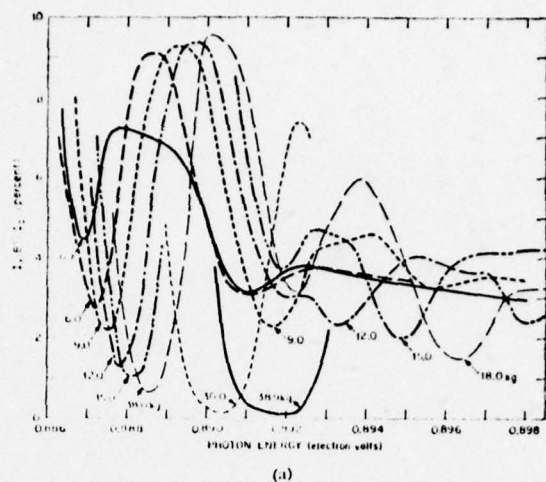


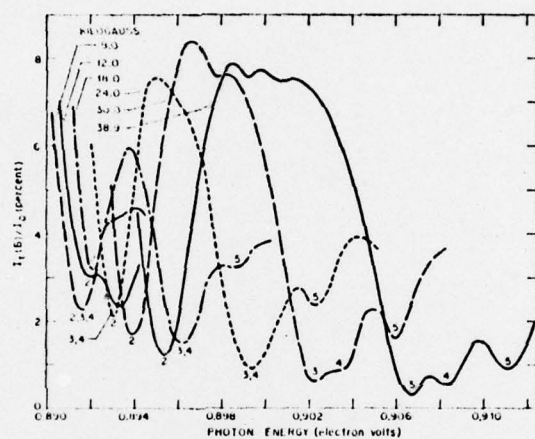
Figure 7 IMPURITY BROADENING OF EXCITON PEAK IN GaSb. (After E. J. Johnson and H Y. Fan.)

$$\mu = \frac{e \langle \tau v^2 \rangle}{200 \text{ m}^* \langle v^2 \rangle}$$

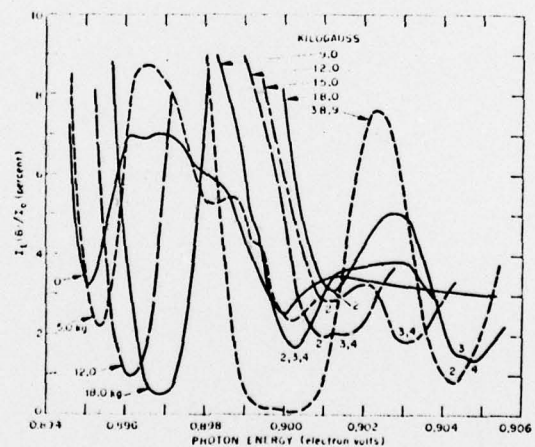
with  $\tau$  the relaxation time



(a)



(b)



(c)

FIG. 8. Detailed magneto-absorption traces for  $E||B$  with the magnetic field intensity as a parameter. The lowest energy exciton line is shown in (a) at  $77^\circ K$ . The higher energy transitions at  $77^\circ K$  are shown in (b). Similar traces for  $1.5^\circ K$  are shown in (c) where the first exciton begins to show a double transmission minimum at 38.9 kilogauss.

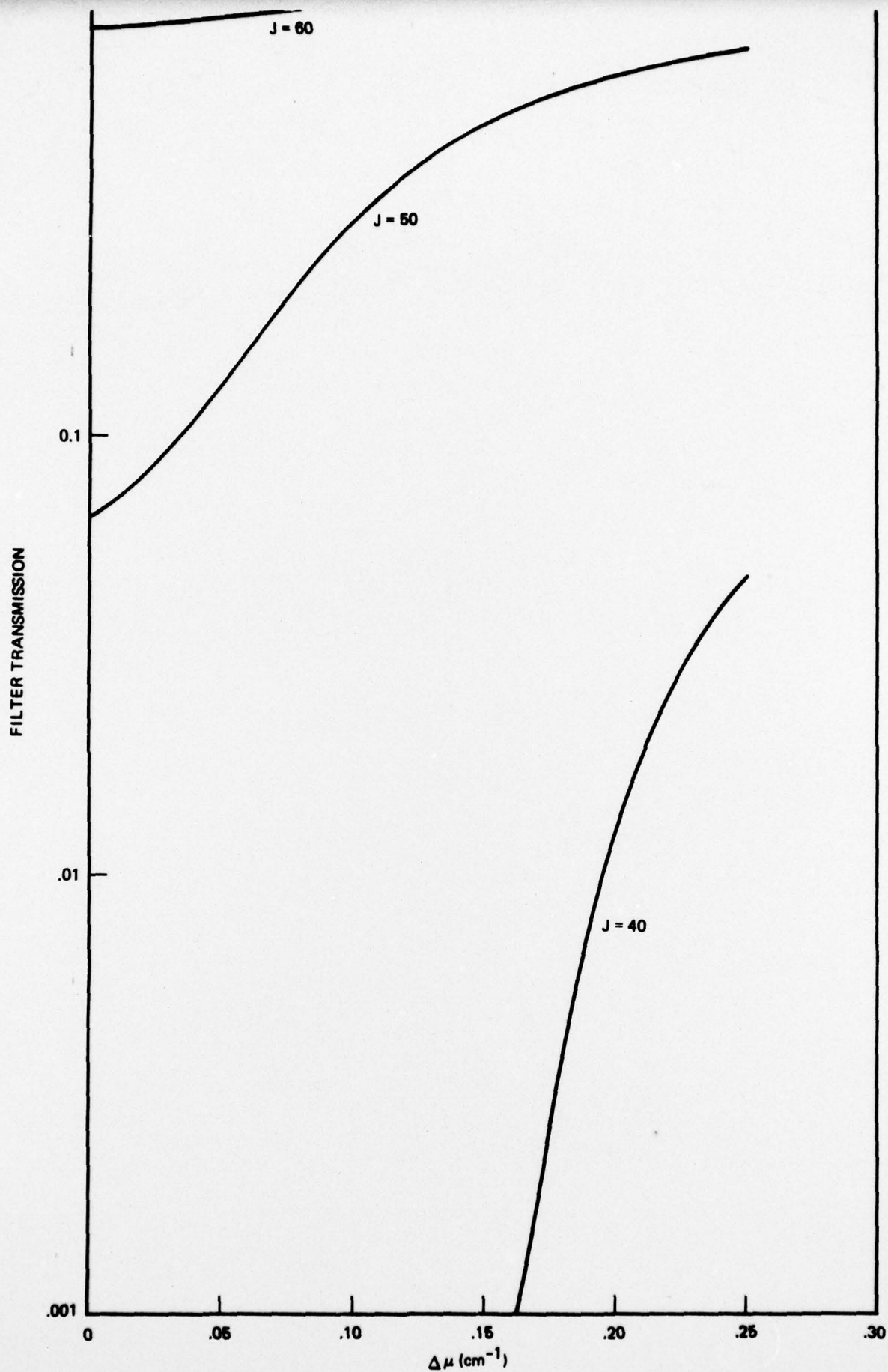


Figure 9 Transmission of a CO<sub>2</sub> Filter at P-1 ctm, T = 200° K, and thickness of 1 cm. The curves refer to three rotational lines in the R branch.



# DISTRIBUTION LIST

JSR-76-31

<u>ORGANIZATION</u>	<u>NO. OF COPIES</u>	<u>ORGANIZATION</u>	<u>NO. OF COPIES</u>
Dr. Joseph W. Chamberlain 18622 Carriage Court Houston, Texas 77058	1	LTC. Charles Lau Advanced Research Projects Agency Strategic Technology Office 1400 Wilson Boulevard Arlington, Virginia 22209	1
Dr. Peter Clark Advanced Research Projects Agency Strategic Technology Office 1400 Wilson Boulevard Arlington, Virginia 22209	1	Dr. Ray L. Leadabrand SRI, International L1053 333 Ravenswood Avenue Menlo Park, CA 94025	1
Major William Cuneo Advanced Research Projects Agency Strategic Technology Office 1400 Wilson Boulevard Arlington, Virginia 22209	1	Dr. Donald M. LeVine SRI, International 1611 North Kent Street Arlington, Virginia 22209	3
Dr. Ruth Davis ODDR&E The Pentagon, Room 3E114 Washington, D.C. 20301	2	Mr. John Morfit P.O. Box 1925 Main Post Office Washington, D.C. 20013	2
Defense Documentation Center Cameron Station Alexandria, Virginia 22314	1	The Honorable Dr. William Perry Director, DDR&E Office of the Secretary of Defense The Pentagon, Room 3E1006 Washington, D.C. 20301	1
Dr. David Elliott SRI, International L2053 333 Ravenswood Avenue Menlo Park, CA 94025	1	Dr. Malvin A. Ruderman 29 Washington Square, West New York, New York 10011	1
Dr. Henry M. Foley Department of Physics Columbia University New York, NY 10027	1	Dr. Donald Scheuch SRI, International D107 333 Ravenswood Avenue Menlo Park, CA 94025	1
Dr. Benjamin Huberman Asst. Director for National Security, International & Space Affairs Office of Science & Technology New Executive Office Bldg., Rm. 3019 Washington, D.C. 20506	1	Dr. Carl Thomas Advanced Research Projects Agency Strategic Technology Office 1400 Wilson Boulevard Arlington, Virginia 22209	1
Mr. Eugene H. Kopf Advanced Research Projects Agency Strategic Technology Office 1400 Wilson Boulevard Arlington, Virginia 22209	1	LTC. William Whitaker Advanced Research Projects Agency 1400 Wilson Boulevard Arlington, Virginia 22209	1